Organic Electronics 14 (2013) 2617–2627

Contents lists available at SciVerse ScienceDirect

Organic Electronics

journal homepage: www.elsevier.com/locate/orgel

Large face to face tetraphenylporphyrin/fullerene nanoaggregates. A DFT study

Ulises Jiménez Castillo, Patricia Guadarrama, Serguei Fomine *

Instituto de Investigaciones en Materiales, Universidad Nacional Autónoma de México, Apartado Postal 70-360, CU, Coyoacán, Mexico DF 04510, Mexico

ARTICLE INFO

Article history:
Received 13 March 2013
Received in revised form 2 May 2013
Accepted 19 May 2013
Available online 11 June 2013

Keywords:
Porphyrin
Fullerene
DFT
Dispersion correction
Reorganization energy

ABSTRACT

Large face to face tetraphenylporphyrin/fullerene nanoaggregates containing up six C60 units and six tetraphenylporphyrin (**H2TPP**) or tetraphenylporphyrinato-zinc (**TPP-Zn**) moieties have been studied using dispersion corrected PBE/def2-SVP level of theory. It has been found that most important contribution to the binding energy between fragments comes from dispersion interactions. The binding energies for Zn containing nanoaggregates are slightly higher than those for metal free ones what is not related to the difference in dispersion contributions to the binding energy but comes from DFT term. Center to center distances for large nanoaggregates are shorter than those for the complexes **H2TPP/C_{60}** and **TPP-Zn/C_{60}** and this effect is more obvious for metal free nanoaggregates. According to the calculations, the band gap of nanoaggregates barely depends on its size being close to 2 eV. The nature of electronic excitations in Zn containing nanoaggregates has strong charge transfer (CT) contribution and does not depend on nanoaggregate size, while for metal free nanoaggregate most of low energy excitations are not CT by nature. Ionization potentials and electron affinities of nanoaggregates depend strongly on their size. Polaron cations are uniformly delocalized over donor **H2TPP** or **TPP-Zn** units, while polaron anions are delocalized over acceptor C_{60} units. The reorganization energies calculated for hole and electron transport decreased linearly with $1/n$ where n is the number of repeating units in nanoaggregate.

1. Introduction

Donor/acceptor functional nanoaggregates has attracted recently much attention as candidates for photovoltaic cells, optoelectronic devices, and applications in artificial photosynthesis [1–6]. The photoinduced electron transfer (PET) from donor to acceptor is the key step for most of those applications. In fact, the core of natural photosynthesis is a multistep PET along the nanoaggregates of donor and acceptors. The most popular building blocks as electron donors in artificial photosynthetic models by obvious reasons are porphyrins, while fullerenes are excellent multielectron acceptors. Porphyrin and fullerene form a very tight complex. Thus, the separation of fullerene carbon and the porphyrin plane is only 2.75 Å, which is notably less than typical separation between molecules experienced π–π interactions which is normally of the order 3.3–3.5 Å. Evidently, the interactions between porphyrin and fullerene are very significant and could be a driving force for the formation of fullerene/porphyrin nanoarrays. In fact, cocrystallization of fullerene with metalloporphyrin or free base porphyrin frequently leads to the formation of an alternating zigzag motif [7]. Up to date a number of porphyrin/fullerene dyads [8–19] triads [20–24] and oligomers involving covalent or noncovalent linkages have been prepared. A recent discovery that among two most common porphyrin/fullerene alignments: face to face and edge to face, the first one allows the PET rates 10 times faster than edge to face orientation [16,25] lead to the synthesis of face to face porphyrin/fullerene nanowires [26]. Therefore, our goal is to study electronic structure of large face

* Corresponding author. Tel.: +52 56224726.
E-mail address: fomine@unam.mx (S. Fomine).

1566-1199/$ - see front matter © 2013 Elsevier B.V. All rights reserved.
http://dx.doi.org/10.1016/j.orgel.2013.05.032

to face porphyrin/fullerene nanowires formed by intermolecular interactions between fullerene and porphyrin moieties using quantum chemistry tools.

The nature of fullerene/porphyrin interactions and PET in face to face dyads have been a subject of intense theoretical studies as well [26–30]. The size of the system and the dominance of weak interactions represent serious challenge for the accurate modeling of such complexes. Thus, reported dimerization energies for C_{60}/tetraphenylporphyrin complex ranged from 11 to −42 kcal/mol, depending on the method used for calculations. According to [28] the use of PBE functional in combination with DZP basis set is able to reproduce the closest center to center distances for C60/tetraphenylporphyrin and C60/tetraphenylporphyrinato-zinc within 0.013 and 0.05 Å, respectively. However, the association energy of −17.3 kcal/mol is very different from that obtained by scaled opposite spin MØller–Plesset method (SOS-MP2) with CBS limit extrapolated basis set (−31.5 kcal/mol), which is probably the best estimation for gas phase association energy of C60/tetraphenylporphyrin complex to date [29]. Interestingly, that different force fields calculations [7,14] give association energies much closer to SOS-MP2 method (28.8–31.9 kcal/mol,) than DFT, suggesting the dominance of dispersion interactions between C_{60} and porphyrin. Therefore, dispersion interactions must be taken into account to model C_{60}/porphyrin arrays. For large systems involving multiple porphyrin and C_{60} molecules where wave function based methods are prohibitively expensive, DFT with explicit or implicit dispersion corrections is the only method of choice.

2. Computational details

Geometry optimization and the energy estimation for C_{60}/tetraphenylporphyrin and C_{60}/tetraphenylporphyrinato-zinc arrays containing up to six donor and six acceptor units were carried out using PBE [31,32] functional and def2-SVP basis set with resolution of identity and Multipole Accelerated Resolution of Identity approximations as implemented in TURBOMOLE 6.4 code [33]. D3 empirical dispersion correction was used for all calculations with PBE functional [34]. The test calculations carried out on C_{60}/tetraphenylporphyrin complex using PBE-D3/def2-SVP model gave the binding energy of 27.0 kcal/mol, reasonably close to the best available estimation of (31.5 kcal/mol) using SOS-MP2 theory. The center to center distances for C_{60}/tetraphenylporphyrin and C_{60}/tetraphenylporphyrinato-zinc were found to be of 2.67 and 2.65 Å, respectively, while the experimental distances are of 2.76 and 2.72 Å [7,35]. We were unable to reproduce data reported in [28] using PBE/DZP model. Both codes, Gaussian 09 [36] and TURBOMOLE 6.4 gave center to center distance for C_{60}/tetraphenylporphyrin complex of 3.03 Å, very different from 2.74 Å reported in [28]. Therefore, we decided to use PBE-D3/def2-SVP model for all calculations. The initial geometries for the C_{60}/tetraphenylporphyrin and C_{60}/tetraphenylporphyrinato-zinc were taken from [28]. Geometries of larger nanoaggregates were constructing from C60/tetraphenylporphyrin and C60/tetraphenylporphyrinato-zinc complexes.

Additionally, periodic boundary condition (PBC) calculations were carried out using Gaussian 09 suit of programs. M06l functional [37] in combination with def2-SVP basis set were applied. M06l functional was shown to produce excellent results for weakly bounded and transition metal complexes and, therefore is suitable for the modeling of C_{60}/porphyrin interactions. No symmetry restriction were imposed during the optimization, restricted and unrestricted DFT were used for closed and open shell systems, respectively. Porphyrin/fullerene nanoaggregates are denoted as **nH2TPP/C_{60}** and **nTPP-Zn/C_{60}**, respectively, where *n* is the number of tetraphenylporphyrin or tetraphenylporphyrinato-zinc units in the aggregate. Plus or minus correspond to cation-radical or anion-radical, respectively.

3. Results and discussion

3.1. Geometry and the binding energies

Optimized geometries of nanoaggregates are shown in Fig. 1. Calculated center to center distances for **H2TPP/C_{60}** and **TPP-Zn/C60** complexes were found to be of 2.67 and 2.65 Å, respectively. For larger aggregates **nH2TPP/C_{60}** where $n = 2$, 4 and 6, center to center distances decrease to 2.54–2.58 Å. Interestingly, that reducing of center to center distances does not observe for Zn-containing nanoaggregates **nTPP-Zn/C_{60}** where center to center distance do not depend on n being of 2.65–2.67 Å for all cases. The decrease of center to center distances for **nH2TPP/C_{60}** aggregates compared to a single complex is related to the introduction of dispersion correction. Dispersion interactions are the long range one, their influence expands beyond the nearest neighbors, thus decreasing the center to center distance compared to **H2TPP/C_{60}.** When no dispersion correction is used for the optimization of **nH2TPP/C_{60}** complexes, the center to center distances are similar for **H2TPP/C_{60}** and **2H2TPP/C_{60}** being of 3.07 Å. In the case of Zn containing nanoaggregates this effect is not observed due to relatively large van der Waals radii of Zn atoms compared to those for the second row elements impeding closer contacts of C_{60} and **H2TPP** fragments.

The PBC calculations carried out using M06l/def2-SVP model gave center to center distances very close to those obtained for **nH2TPP/C_{60}** and **nTPP-Zn/C_{60}** oligomers with PBE-D3/def2-SVP model: 2.59 and 2.66 Å, for **poly-H2TPP/C_{60}** and **poly-TPP-Zn/C_{60},** respectively. Both methods take into accounts dispersion, leading to close intermolecular distances.

The calculated binding energies of nanoaggregates are listed in Table 1. The binding energies of Zn containing nanoaggregates are only slightly higher compared to those of **nH2TPP/C_{60}** ones. Total binding energies increases greatly with size of nanoaggregate, however, reduced binding energies are almost constant being of 25–27 kcal/mol for **nH2TPP/C_{60}** and 27–28 kcal/mol for **nTPP-Zn/C_{60}.** When comparing the contribution of dispersion interactions to the total binding energy it is clearly seen that

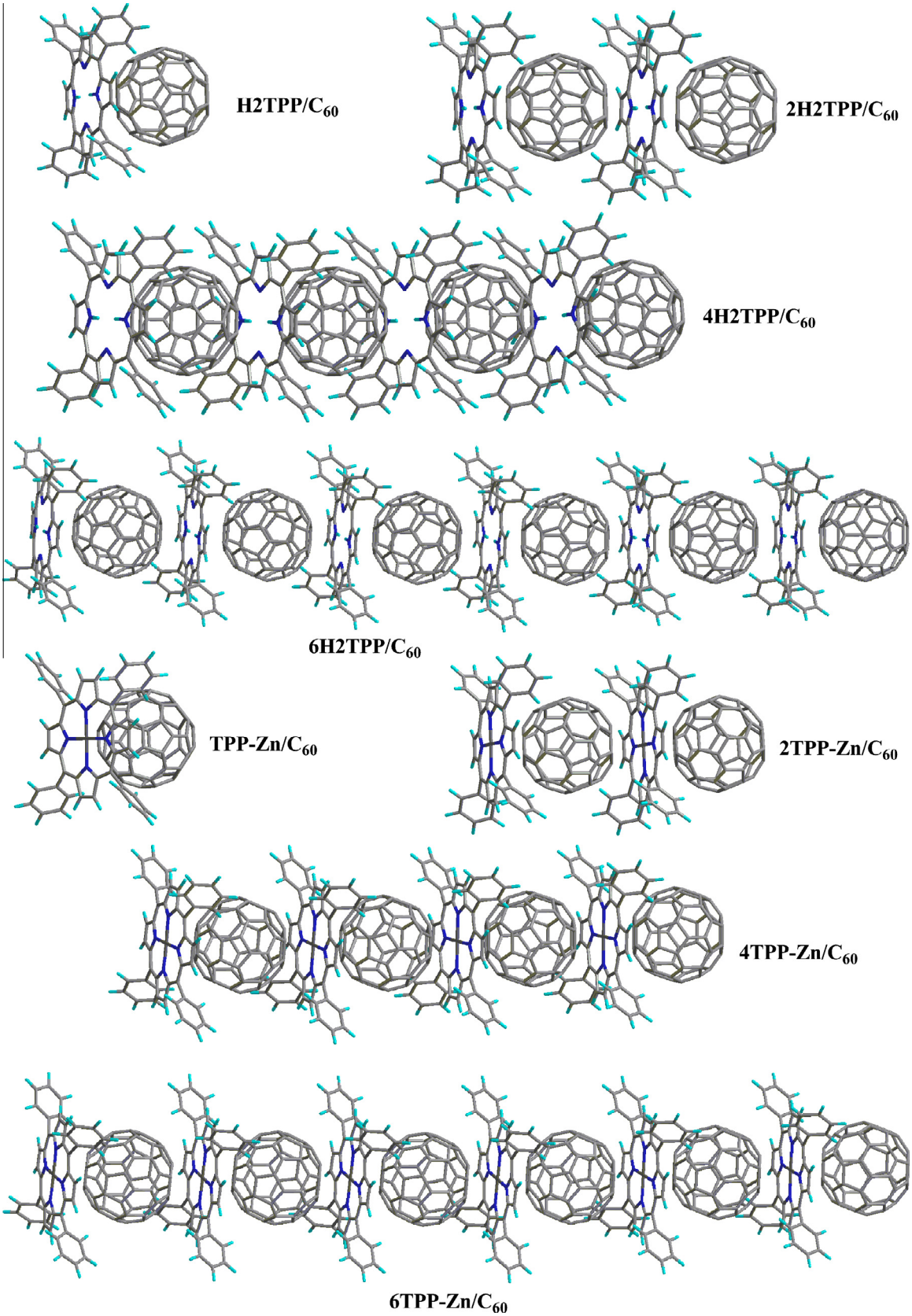

Fig. 1. PBE-D3/def2-SVP optimized geometries of nanoaggregates.

Table 1
Vertical (v) and adiabatic (a) ionization potentials (**IP**), electron affinities (**EA**), reorganization energies for hole (λ_+) and electron (λ_-) transport, band gaps (E_g), **S0 → S1** excitation energies (eV) of studied nanoaggregates. Total binding energies (E_{tot}) calculated using PBE + D model and the corresponding contributions from dispersion energy (E_{disp}) and dispersion uncorrected PBE energy (E_{dft}) (kcal/mol).

Complex	IP_v	IP_a	EA_v	EA_a	λ_+	λ_-	E_g	S0 → S1	E_{tot}	E_{disp}	E_{dft}
H2TPP/C_{60}	6.10	6.06	2.50	2.57	0.07	0.14	1.76	2.02	27.0	27.3	−0.3
2H2TPP/C_{60}	5.68	5.66	2.87	2.91	0.04	0.08	1.80	1.98	77.4 (25.8)	76.6 (25.5)	0.8 (0.3)
4H2TPP/C_{60}	5.35	5.34	3.14	3.17	0.02	0.05	1.77	1.98	178.2 (25.4)	174.9 (25.0)	3.3 (0.5)
6H2TPP/C_{60}	5.20	5.20	3.29	3.29	0.01	0.02	1.76	–	279.2 (25.4)	272.9 (24.8)	6.3 (0.6)
poly-H2TPP/C_{60}	–	–	–	–	–	–	1.92	–	–	–	–
TPP-Zn/C_{60}	6.06	6.00	2.62	2.71	0.10	0.18	1.69	2.00	29.3	27.3	2.0
2TPP-Zn/C_{60}	5.64	5.62	3.01	3.05	0.04	0.08	1.66	2.00	84.3 (28.1)	75.8 (25.5)	8.5 (2.8)
4TPP-Zn/C_{60}	5.31	5.30	3.30	3.32	0.02	0.04	1.63	2.01	194.2 (27.7)	172.6 (24.7)	21.6 (3.1)
6TPP-Zn/C_{60}	5.16	5.16	3.44	3.44	0.01	0.01	1.61	–	304.2 (27.7)	270.7 (24.6)	33.5 (3.0)
poly-TPP-Zn/C_{60}	–	–	–	–	–	–	1.69	–	–	–	–
C_{60}	7.40	7.34	2.60	2.66	0.11	0.11	–	–	–	–	–
H2TPP	6.12	6.07	1.48	1.56	0.09	0.12	–	–	–	–	–
TPP-Zn	6.16	6.11	1.42	1.48	0.09	0.13	–	–	–	–	–

dispersion accounts for more than 90% of total binding energy of nanoaggregates and in the case of **nH2TPP/C_{60}** approaches 100%. This results is in line with recent high level calculations [29] where the dominance of dispersion forces for **H2TPP/C_{60}** has been suggested and it is the strong dispersion interactions that bring C_{60} and TPP in close proximity (inside the van der Waals contact distance). The data from Table 1 demonstrate that the dispersion term is similar for the metal free and Zn containing nanoaggregates and the difference of the binding energies between **nH2TPP/C_{60}** and **nTPP-Zn/C_{60}** is due to pure DFT contribution.

3.2. Excited state properties

For the determination of the band gap (E_g) of nanoaggregates two different methods have been used. The first one defines the band gap as simple HOMO–LUMO energy difference taken from B3LYP/def2-SVP single point calculations. B3LYP functional produces reliable results for estimation of E_g in conjugated polymers [38]. Second one is the direct calculation of the lowest excited state energy using time dependent (TD) implementation of CAM-B3LYP functional [39]. CAM-B3LYP functional is especially designed to deal with electronic transition in donor–acceptor systems. Due to the size of the systems, direct calculations of the excitation energies were possible only for nanoaggregates containing up to four repeating units; **4H2TPP/C_{60}** and **4TPP-Zn/C_{60}** (Table 1). According to HOMO–LUMO method, E_g does not depend on n for **nH2TPP/C_{60}** nanoaggregates being in the range of 1.76–1.80 eV, for infinite **poly-H2TPP/C_{60}** a reasonably close value of 1.92 eV was obtained. This is rather close to the estimations for S0 → S1 transition of **H2TPP/C_{60}** dyad using TD-PBE method (1.77 eV) [30]. TD-CAM-B3LYP estimation of S0 → S1 transition energy for **nH2TPP/C_{60}** is in line with HOMO–LUMO difference suggesting no dependence of S0 → S1 energy on the number of repeating units in nanoaggregates. TD-DFT gives slightly higher values for E_g than HOMO–LUMO energy difference (1.98–2.02 eV).

For Zn containing nanoaggregates HOMO–LUMO energy difference gives E_g from 1.69 eV for **TPP-Zn/C_{60}** to 1.61 eV for **6TPP-Zn/C_{60}**. For **poly-4TPP-Zn/C_{60}** E_g was found to be of 1.69 eV, very close to that calculated for oligomers. Again, this estimation is very close to the S0 → S1 excitation energies calculated with TD-PBE model (1.68 eV) for **TPP-Zn/C_{60}** dyad [30]. TD-CAM-B3LYP predicts S0 → S1 transition energies for **nTPP-Zn/C_{60}** to be very close to 2 eV, with no dependence on n similar to that for **nH2TPP/C_{60}**. However, the nature of those transitions is very different for two types of nanoaggregates. Figs. 2 and 3 show natural transition orbitals (NTOs) [40] for some of the low singlet transitions in **nH2TPP/C_{60}** and **nTPP-Zn/C_{60}**. As seen, all S0 → S1 transitions of **nH2TPP/C_{60}** show no appreciable charge transfer (CT) character. Thus, for **H2TPP/C_{60}** and **2H2TPP/C_{60}** the first excitations with significant charge transfer character are S0 → S2 and S0 → S4, respectively. On the other hand, all S0 → S1 excitations in Zn containing nanoaggregates show significant (CT) character (Fig. 3). Moreover, in the case of **nTPP-Zn/C_{60}** nanoaggregates for $n = 1$ all three lowest excited states are the CT states, while for $n = 2$ all four calculated lowest excited states are CT states. For $n = 4$, only the lowest excited state has been determined due to the size of nanoaggregate and it was found to have a strong CT character. The fact that E_g of nanoaggregates does not depends on its size suggests that the units are optically isolated and excitations are local by nature. Strong CT character of excitations of **nTPP-Zn/C_{60}** nanoaggregates is promising for possible photovoltaic applications.

3.3. Ionization potentials, electron affinities and reorganization energies

Unlike the lowest excitation energy, which is barely depends on the length of nanoaggregates, the ionization potentials (IP's) and the electron affinities (EA's) of **nH2TPP/C_{60}** and **nTPP-Zn/C_{60}** depend on n (Table 1) suggesting that both positive and positive charges are delocalized over the entire nanoaggregate. If for dyads **H2TPP/C_{60}** and **TPP-Zn/C_{60}** IP's and EA's are close to that for **H2TPP**, **TPP-Zn** and C_{60}, respectively, for larger nanoaggregates IP's are notably lower and EA's are higher than those of individual donors and acceptors. Thus, **6H2TPP/C_{60}** and

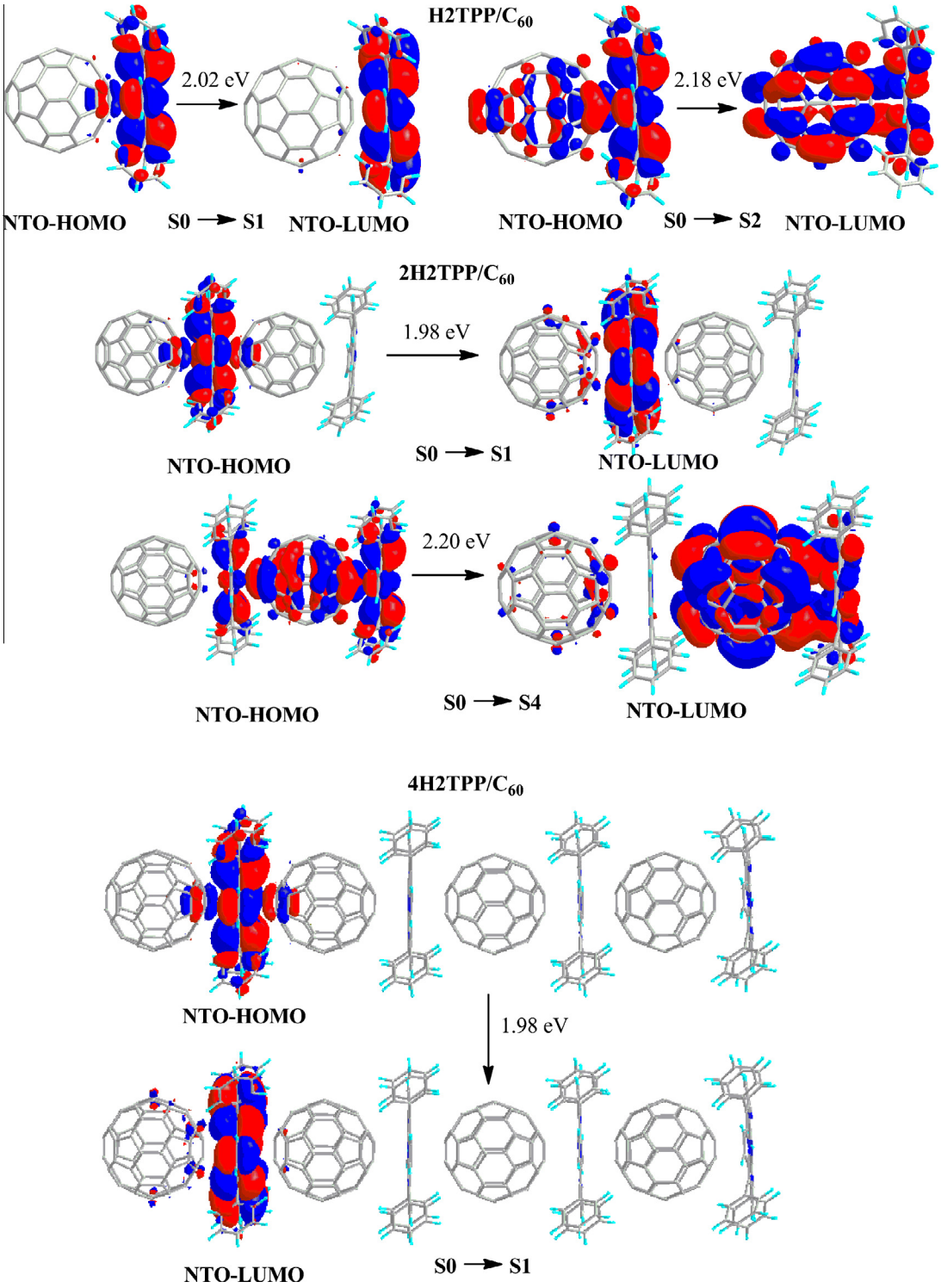

Fig. 2. Natural transition orbitals (NTOs) for electronic transitions in **nH2TPP/C_{60}** nanoaggregates.

6TPP-Zn/C_{60} have their IP's close to 5 eV, which is very similar to that reported for IP_a of polythiophene [41], while their estimated EA's are higher than 3 eV, which is higher than that of C_{60} [42]. Although **TPP-Zn** has higher IP's and lower EA's compared to **H2TPP**, the IP's of Zn containing nanoaggregates are lower and EA's are higher compared to **nH2TPP/C_{60}**. This effect is due to the fact that metal atoms allow better orbital overlap between C_{60} and

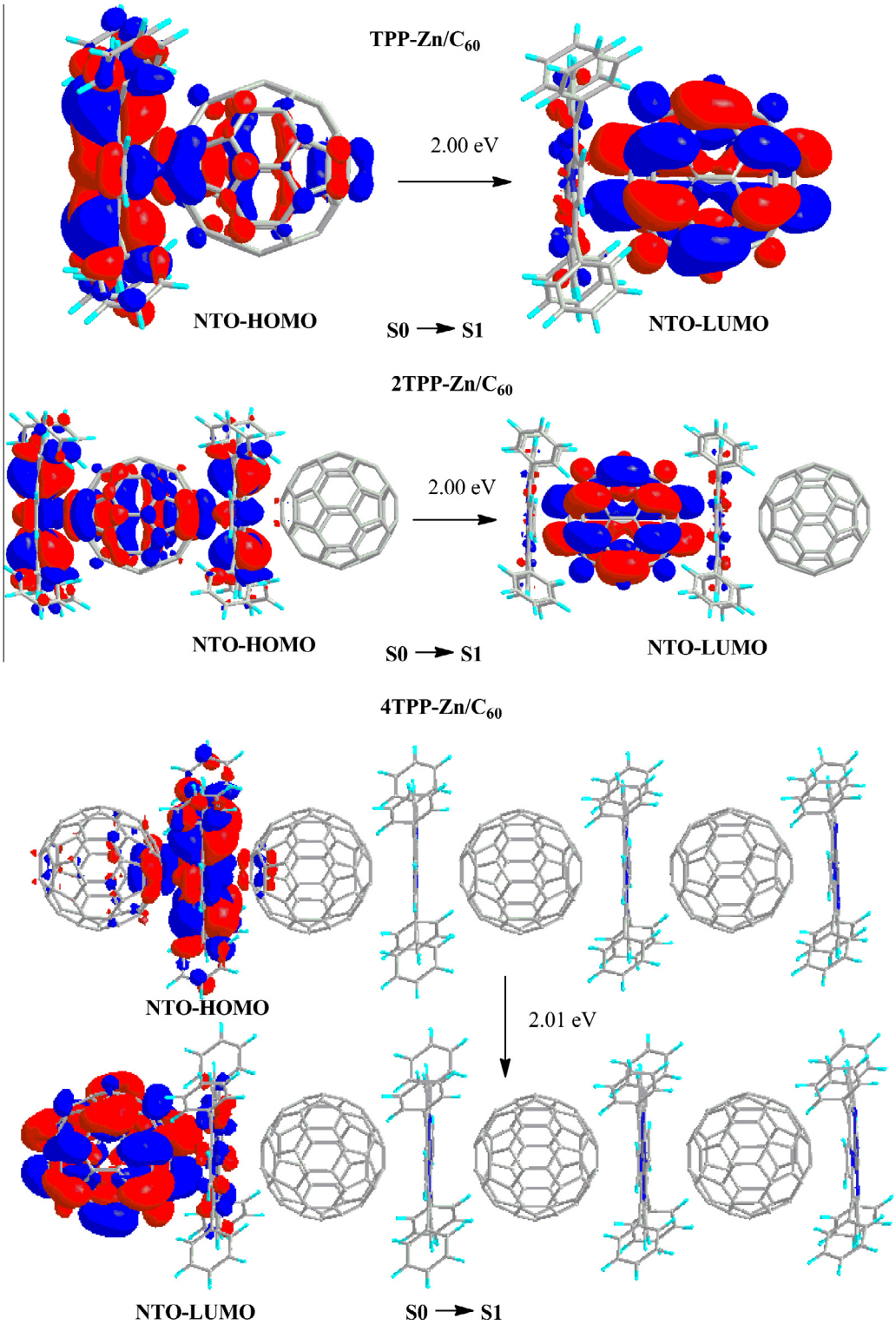

Fig. 3. Natural transition orbitals (NTOs) for electronic transitions in **nTPP-Zn/C_{60}** nanoaggregates.

H2TPP fragments facilitating polaron delocalization along the nanoaggregate. Figs. 4 and 5 show polaron delocalization in cation and anion radicals of nanoaggregates, respectively. In a polaron the charge is associated with unpaired electron, therefore, polaron delocalization can be visualized as unpaired electron density. As seen from

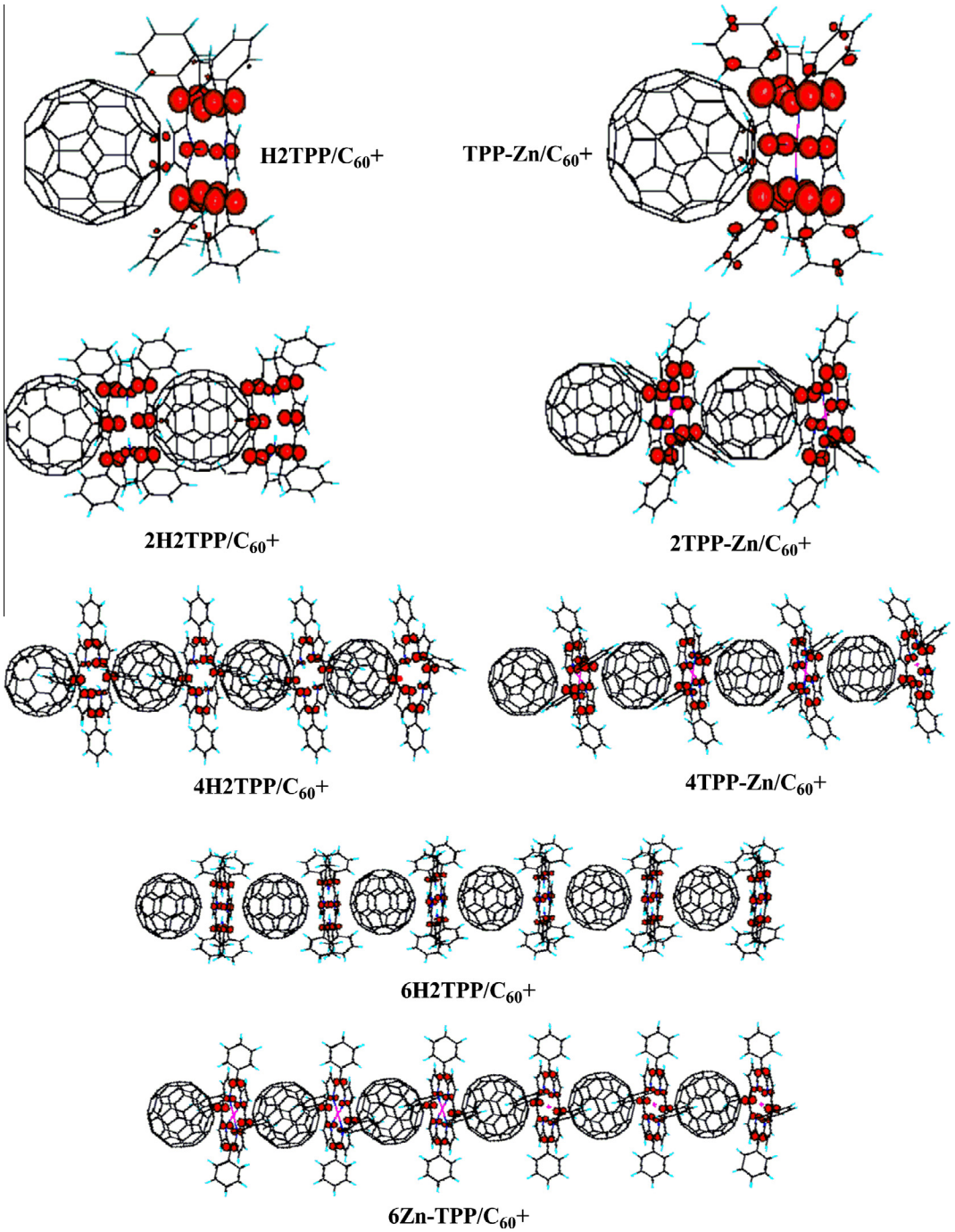

Fig. 4. Delocalization of polaron cations in **nH2TPP/C_{60}** nanoaggregates.

Fig. 4 polaron cation is delocalized uniformly over the nitrogen atoms and methyne carbons of donor **TPP** units, explaining decreasing of IP's with size of nanoaggregates. Phenyl substituents and Zn ions of Zn containing nanoaggregates do not participate significantly in the delocalization of polaron cation. On the other hand, in the case of polaron anions, the delocalization only involves acceptor C_{60} fragments and the most of polaron anion is located at the terminal fullerene moieties, while internal C_{60} fragments participate less in the delocalization of polaron anion. This effect can be appreciated for **4H2TPP/C_{60}**, **4TPP-Zn/C_{60}**, **6H2TPP/C_{60}** and **6TPP-Zn/C_{60}**. The increase of adiabatic EA's with n for nanoaggregates is about 0.12 eV less than decrease of IP's due to less delocalized polaron anions (Table 1).

The electron attachment or electron detachment changes the geometry of nanoaggregates. This effect is the most important for small nanoaggregates, while for

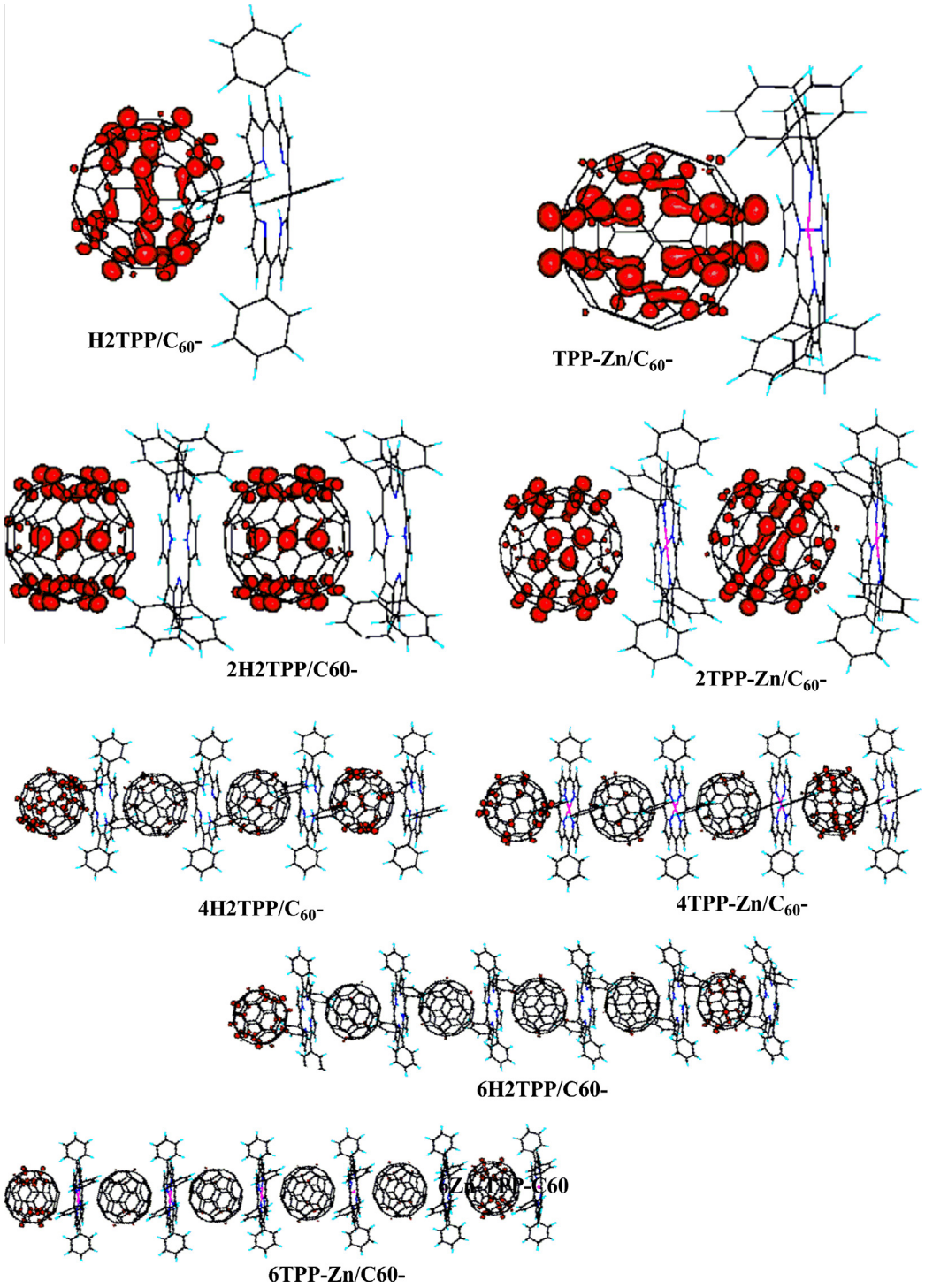

Fig. 5. Delocalization of polaron anions in **nTPP-Zn/C_{60}** nanoaggregates.

the nanoaggregates with $n = 4$ and 6 it is almost imperceptible due to delocalization of the positive or negative charges. The electron detachment causes decrease of center to center distances to 2.57 Å in **H2TPP/C_{60}+** and **TPP-Zn/C_{60}+** from 2.67 and 2.65 Å, respectively. Similar effect takes place on electron attachment; center to center distance decreases in **H2TPP/C_{60}**− and **TPP-Zn/C_{60}**− to 2.64 and 2.56 Å, respectively. Since dispersion interactions are the most important for **TPP/C_{60}** systems, the increase of polarizability due to the formation of open shell system

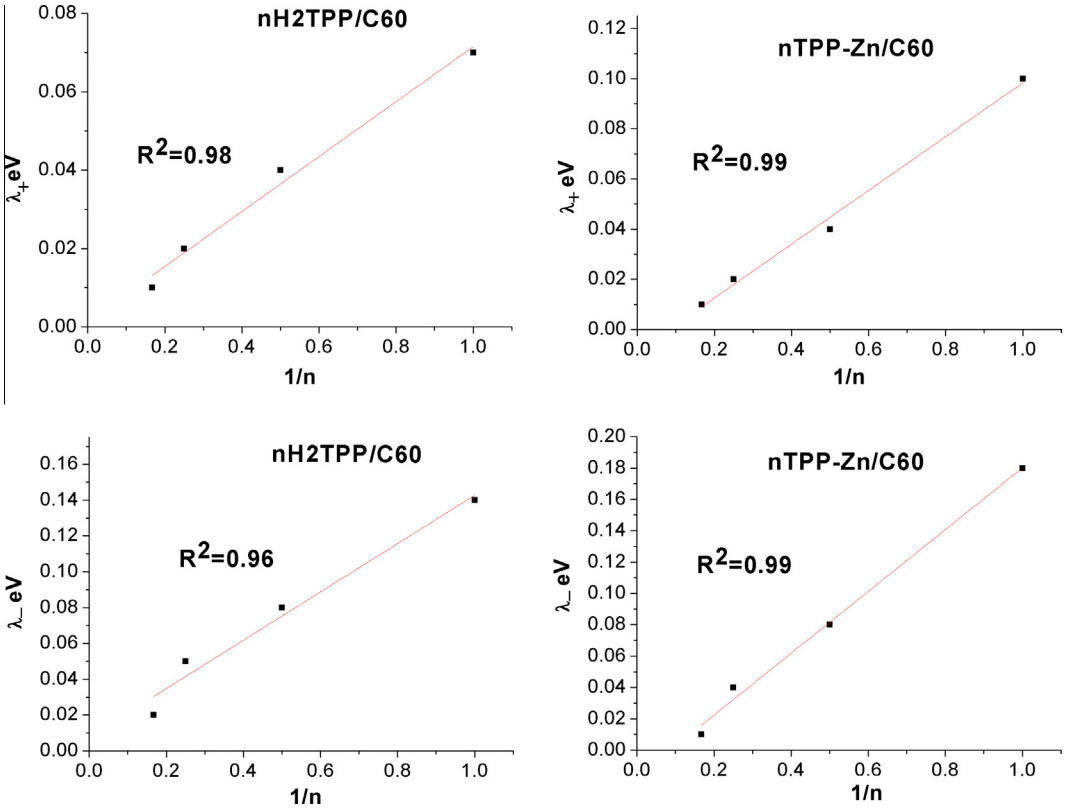

Fig. 6. Relaxation energies for hole (λ_+) and electron transport (λ_-) of nanoaggregates versus reciprocal number of repeating units in nanoaggregates.

(polaron cation or polaron anion) increases the dispersion interactions between donor (**TPP**) and acceptor (C_{60}) fragments, thus shortening center to center distance.

An important point in understanding conductivity of **nTPP/C$_{60}$** nanoaggregates is to characterize structural factors essentials in the charge transfer rates. Thus, it has been demonstrated that the solid-state the hole mobility in arylamines is related to the internal reorganization energy λ [43–45]. For the hole mobility the reorganization energy (λ_+) can be estimated as follows as long as local vibronic coupling is dominated:

$$\lambda_+ = (E_n^+ - E_n) + (E_+^n - E_+)$$

E_n and E_+ are the energies of the neutral and cationic species in their lowest energy geometries, respectively, while E_n^+ and E_+^n are the energies of the neutral and cationic species with the geometries of the cation and neutral species, respectively. For the electron transport the reorganization energy is defined similarly:

$$\lambda_- = (E_n^- - E_n) + (E_-^n - E_-)$$

In this case E_n and E_- are the energies of the neutral and anion species in their lowest energy geometries, respectively, while E_n^- and E_-^n are the energies of the neutral and anion species with the geometries of the cation and neutral species, respectively. Fig. 6 and Table 1 summarized calculated λ_+ and λ_- for **nTPP-Zn/C$_{60}$** and **nH2TPP/C$_{60}$** and the corresponding individual donors and acceptors (**H2TPP**, **TPPZn** and C_{60}). The relaxation energies for nanoaggregates decrease with n, becoming smaller than those for individual donors and acceptors already for $n = 2$. There is a linear correlation between λ and $1/n$ with $R^2 > 0.95$ for both hole and electron transport. It is noteworthy that the same behavior has been found for reorganization energies of polythiophene and polyselenophene [46]. All other things being equal the hole mobilities in **nTPP-Zn/C$_{60}$** and **nH2TPP/C$_{60}$** nanoaggregates are higher than electron mobility since $\lambda_+ < \lambda_-$. Although for small n the reorganization energies are lower for metal free **nTPP-C60** nanoaggregates the extrapolation show that for **nTPP-Zn/C$_{60}$,** λ reaches 0 for n about 10 while for **nH2TPP/C$_{60}$** zero reorganization energy is reached (if any) for longer nanoaggregates. However, in any case the calculated reorganization energies for both hole and electron mobilities are very small for long nanoaggregates and they should have high charge mobilities provided the electron coupling between C_{60} and **TPP** fragments is sufficiently strong.

4. Conclusions

The nature of binding in **nH2TPP/C$_{60}$** and **nTPP-Zn/C$_{60}$** nanoaggregates is mostly dispersion. Therefore, taking into account those interactions is of primary importance to describe correctly interactions between porphyrin and fullerene. For both types of nanoaggregates, **nH2TPP/C$_{60}$** and **nTPP-Zn/C$_{60}$** the contribution of dispersion interaction to the binding energy is nearly the same and the difference

in binding energy is totally related to DFT contribution. Calculated center to center distances for **nH2TPP/C_{60}** and **nTPP-Zn/C_{60}** nanoaggregates are shorter than those for the complexes **H2TPP/C_{60}** and **TPP-Zn/C_{60}** and this effect is more obvious for metal free nanoaggregates. According to the calculations E_g of nanoaggregates barely depends on n. This conclusion agrees with both, the estimation of E_g as HOMO–LUMO energy difference from single point B3LYP calculations and direct calculation of lowest excitation energies using TD-CAM-B3LYP theory. While HOMO–LUMO energy difference predict that the presence of Zn marginally decrease E_g, according to TD-DFT, E_g for all nanoaggregates is close to 2 eV. The nature of electronic excitations in **nTPP-Zn/C_{60}** nanoaggregates has strong CT contribution where the particle orbital is located at **TPP-Zn** moiety and the hole orbital an C_{60} one, for metal free nanoaggregate most of low energy excitations are not CT by nature. Unlike E_g, IP's and EA's of nanoaggregates depend strongly on n and being close for **nH2TPP/C_{60}** and **nTPP-Zn/C_{60}** nanoaggregates. Polaron cations are uniformly delocalized over donor **H2TPP** or **TPP-Zn** units, while polaron anions are delocalized over acceptor C_{60} units. Calculated reorganization energies for hole and electron transport (λ_+ and λ_-, respectively) decreased linearly with $1/n$. In the case of **nTPP-Zn/C_{60}** the extrapolated λ_+ and λ_- approach zero for n about 10 while for less rigid metal free nanoaggregates this in not the case. For both **nH2TPP/C_{60}** and **nTPP-Zn/C_{60}** nanoaggregates $\lambda_+ < \lambda_-$.

Acknowledgment

The authors acknowledge the financial support from PAPIIT (Grant IN-100712/24).

Appendix A. Supplementary material

Supplementary data associated with this article can be found, in the online version, at http://dx.doi.org/10.1016/j.orgel.2013.05.032.

References

[1] C.J. Brabec (Ed.), Organic Photovoltaics: Concepts and Realization, Springer, Berlin, 2003.
[2] C.J. Brabec, V. Dyakonov, U. Scherf (Eds.), Organic Photovoltaics: Materials, Device Physics, and Manufacturing Technologies, Wiley VCH, Weinheim, 2008.
[3] N.R. Armstrong, W.N. Wang, D.M. Alloway, D. Placencia, E. Ratcliff, M. Brumbach, Organic/organic heterojunctions: organic light emitting diodes and organic photovoltaic devices, Macromol. Rapid Commun. 30 (2009) 717–731.
[4] A. de la Escosura, M.V. Martinez-Diaz, T. Torres, R.H. Grubbs, D.M. Guldi, H. Neugebauer, C. Winder, M. Drees, N.S. Sariciftci, New donor–acceptor materials based on random polynorbornenes bearing pendant phthalocyanine and fullerene units, Asian J. Chem. 1 (2006) 148–154.
[5] G. Bottari, G. de la Torre, D.M. Guldi, T. Torres, Covalent and noncovalent phthalocyanine–carbon nanostructure systems: synthesis, photoinduced electron transfer, and application to molecular photovoltaics, Chem. Rev. 110 (2010) 6768–6816.
[6] S. Gunes, H. Neugebauer, N.S. Sariciftci, Conjugated polymer-based organic solar cells, Chem. Rev. 107 (2007) 1324–1338.
[7] P.D.W. Boyd, M.C. Hodgson, L. Chaker, C.E.F. Rickard, A.G. Oliver, P.J. Brothers, R. Bolskar, F.S. Tham, C.A. Reed, Selective supramolecular fullerene porphyrin interactions, J. Am. Chem. Soc. 121 (1999) 10487–10495.
[8] J.L. Segura, N. Martin, Fullerene dimers, Chem. Soc. Rev. 29 (2000) 13–25.
[9] M.D. Meijer, G.P.M. van Klink, G. van Koten, Metal-chelating capacities attached to fullerenes, Coord. Chem. Rev. 230 (2002) 141–163.
[10] D.M. Guldi, Fullerene–porphyrin architectures; photosynthetic antenna and reaction center models, Chem. Soc. Rev. 31 (2002) 22–36.
[11] A. Satake, Y. Kobuke, Dynamic supramolecular porphyrin systems, Tetrahedron 61 (2005) 13–41.
[12] T. Konishi, A. Ikeda, S. Shinkai, Supramolecular design of photocurrent-generating devices using fullerenes aimed at modelling artificial photosynthesis, Tetrahedron 61 (2005) 4881–4899.
[13] G. Kodis, Y. Terazono, P.A. Liddell, J. Andreasson, V. Garg, M. Hambourger, T.A. Moore, A.L. Moore, D. Gust, Energy and photoinduced electron transfer in a wheel-shaped artificial photosynthetic antenna-reaction center complex, J. Am. Chem. Soc. 128 (2006) 1818–1827.
[14] D.I. Schuster, P.D. Jarowski, A.N. Kirschner, S.R. Wilson, Molecular modelling of fullerene–porphyrin dyads, Mater. Chem. 12 (2002) 2041–2047.
[15] D. Gust, T.A. Moore, A.L. Moore, S.J. Lee, E. Bittersmann, D.K. Luttrull, A.A. Rehms, J.M. DeGraziano, X.C. Ma, Efficient multistep photoinitiated electron transfer in a molecular pentad, Science 248 (1990) 199–201.
[16] F. D'Souza, E. Maligaspe, P. Karr, A.L. Schumacher, M. El Ojaimi, C.P. Gros, J.M. Barbe, K. Ohkubo, S. Fukuzumi, Face-to-face pacman-type porphyrin–fullerene dyads: design, synthesis, charge-transfer interactions, and photophysical studies, Chem. Eur. J. 14 (2008) 674–681.
[17] S.A. Vail, P.J. Krawczuk, D.M. Guldi, A. Palkar, L. Echegoyen, C.J.P. Tome, M.A. Fazio, D.I. Schuster, Energy and electron transfer in polyacetylene-linked zinc–porphyrin–[60]fullerene molecular wires, Chem. Eur. J. 11 (2005) 3375–3388.
[18] S.A. Vail, D.I. Schuster, D.M. Guldi, M. Isosomppi, N. Tkachenko, H. Lemmetyinen, A. Palkar, L. Echegoyen, X. Chen, J.Z.H. Zhang, Energy and electron transfer in β-alkynyl-linked porphyrin–[60]fullerene dyads, J. Phys. Chem. B 110 (2006) 14155–14166.
[19] S. MacMahon, R. Fong II, P.S. Baran, I. Safonov, S.R. Wilson, D.I. Schuster, Synthetic approaches to a variety of covalently linked porphyrin–fullerene hybrids, J. Org. Chem. 66 (2001) 5449–5455.
[20] N. Armaroli, G. Marconi, L. Echegoyen, J.P. Bourgeois, F. Diederich, Charge-transfer interactions in face-to-face porphyrin-fullerene systems: solvent-dependent luminescence in the infrared spectral region, Chem. Eur. J. 6 (2000) 1629–1645.
[21] C. Luo, D.M. Guldi, H. Imahori, K. Tamaki, Y. Sakata, Sequential energy and electron transfer in an artificial reaction center: formation of a long-lived charge-separated state, J. Am. Chem. Soc. 122 (2000) 6535–6551.
[22] H. Imahori, K. Tamaki, D.M. Guldi, C. Luo, M. Fujitsuka, O. Ito, Y. Sakata, S. Fukuzumi, Modulating charge separation and charge recombination dynamics in porphyrin–fullerene linked dyads and triads: marcus-normal versus inverted region, Am. Chem. Soc. 123 (2001) 2607–2617.
[23] H.J. Kim, K.M. Park, T.K. Ahn, S.K. Kim, K.S. Kim, D. Kim, H.J. Kim, Novel fullerene–porphyrin–fullerene triad linked by metal axial coordination: Synthesis, X-ray crystal structure, and spectroscopic characterizations of *trans*-bis([60]fullerenoacetato)tin(IV) porphyrin, Chem. Commun. (2004) 2594–2595.
[24] A.S.D. Sandanayaka, K. Ikeshita, Y. Araki, N. Kihara, Y. Furusho, T. Takata, O. Ito, Photoinduced electron- and energy-transfer processes of [60]fullerene covalently bonded with one and two zinc porphyrin(s): effects of coordination of pyridine and diazabicyclooctane to Zn atom, J. Mater. Chem. 15 (2005) 2276–2287.
[25] D.M. Guldi, C.P. Luo, M. Prato, A. Troisi, F. Zerbetto, M. Scheloske, E. Dietel, W. Bauer, A. Hirsch, Parallel (face-to-face) versus perpendicular (edge-to-face) alignment of electron donors and acceptors in fullerene porphyrin dyads: the importance of orientation in electron transfer, J. Am. Chem. Soc. 123 (2001) 9166–9167.
[26] H. Xu, J. Zheng, Face-to-face alignment of porphyrin/fullerene nanowires linked by axial metal coordination macromol, Chem. Phys 211 (2010) 2125–2131.
[27] M.J. Shephard, M.N. Paddon-Row, The porphyrin-C60 non-bonded interaction: an ab initio MO and DFT study, J. Porphyrins Phthalocyanines 6 (2002) 783–794.

[28] Y.B. Wang, Z.Y. Lin, Supramolecular interactions between fullerenes and porphyrins, J. Am. Chem. Soc. 125 (2003) 6072–6073.
[29] Y. Jung, M. Head-Gordon, A fast correlated electronic structure method for computing interaction energies of large van der Waals complexes applied to the fullerene–porphyrin dimer, Phys. Chem. Chem. Phys. 8 (2006) 2831–2840.
[30] R.R. Zope, M. Olguin, T. Baruah, Charge transfer excitations in cofacial fullerene–porphyrin complexes, J. Chem. Phys. 137 (2012) 084317.
[31] J.P. Perdew, K. Burke, M. Ernzerhof, Generalized gradient approximation made simple, Phys. Rev. Lett. 77 (1996) 3865–3868.
[32] J.P. Perdew, K. Burke, M. Ernzerhof, Errata: generalized gradient approximation made simple, Phys. Rev. Lett. 78 (1997) 1396.
[33] TURBOMOLE V6.4 2012, a development of University of Karlsruhe and Forschungszentrum Karlsruhe GmbH, 1989–2007, TURBOMOLE GmbH, since 2007, available from www.turbomole.com.
[34] S. Grimme, J. Antony, S. Ehrlich, H. Krieg, A consistent and accurate ab initio parametrization of density functional dispersion correction (DFT-D) for the 94 elements H-Pu, J. Chem. Phys. 132 (2010) 154104.
[35] M.M. Olmstead, D.A. Costa, K. Maitra, B.C. Noll, S.L. Phillips, P.M. Van Calcar, A.L. Balch, Interaction of curved and flat molecular surfaces. the structures of crystalline compounds composed of fullerene (C_{60}, $C_{60}O$, C_{70}, and $C_{120}O$) and metal octaethylporphyrin units, J. Am. Chem. Soc. 121 (1999) 7090–7097.
[36] Gaussian 09, Revision C.01, M. J. Frisch, et al., Gaussian, Inc., Wallingford CT, 2010.
[37] Y. Zhaoand, D.G. Truhlar, A new local density functional for main-group thermochemistry, transition metal bonding, thermochemical kinetics, and noncovalent interactions, J. Chem. Phys. 125 (2006) 194101.
[38] S. Yang, M. Kertesz, Theoretical design of low band gap conjugated polymers through ladders with acetylenic crosspieces, Macromolecules 40 (2007) 6740–6747.
[39] T. Yanai, D.P. Tew, N.C. Handy, A new hybrid exchange–correlation functional using the coulomb-attenuating method (CAM-B3LYP), Chem. Phys. Lett. 393 (2004) 51–57.
[40] Richard L. Martin, Natural transition orbitals, J. Chem. Phys. 118 (2003) 4775–4777.
[41] U. Salzner, P.G. Pickup, R.A. Poirier, J.B. Lagowski, An accurate method for obtaining band gaps in conducting polymers using a DFT/hybrid approach, J. Phys. Chem. A 102 (1998) 2572–2578.
[42] X.B. Wang, Ch-Fan Ding, L.S. Wang, High resolution photoelectron spectroscopy of $C60^-$, Chem. Phys. 110 (1999) 8217–8220.
[43] B.C. Lin, C.P. Cheng, Z.P.M. Lao, Reorganization energies in the transports of holes and electrons in organic amines in organic electroluminescence studied by density functional theory, J. Phys. Chem. A 107 (2003) 5241.
[44] M. Malagoli, J.L. Brédas, Density functional theory study of the geometric structure and energetics of triphenylamine-based hole-transporting molecules, Chem. Phys. Lett. 327 (2000) 13–17.
[45] K. Sakanoue, M. Motoda, M. Sugimoto, S. Sakaki, A molecular orbital study on the hole transport property of organic amine compounds, J. Phys. Chem. A 103 (1999) 5551–5556.
[46] S.S. Zade, M. Bendikov, Study of hopping transport in long oligothiophenes and oligoselenophenes: dependence of reorganization energy on chain length, Chem. Eur. J. 14 (2008) 6734–6741.